

Supporting Information

Insight into the Role of Nitrogen in N-Doped Ordered Mesoporous Carbons for Spontaneous Non-covalent Attachment and Electrografting of Redox Active Materials

Nasim Shamsvand^a, Fahimeh Varmaghani^{*a,b}, Babak Karimi^{*a,b}, Hamzeh Hassanaki

*^aDepartment of Chemistry, Institute for Advanced Studies in Basic Sciences (IASBS), Zanjan
45137-66731, Iran*

*^bResearch Center for Basic Sciences and Modern Technologies (RBST), Institute for Advanced
Studies in Basic Sciences (IASBS), Zanjan 45137-66731, Iran*

Contents

Fig. S1. The effect of scan rate on the voltammogram of catechol on GIOMC/GCE	Page 3
Fig. S2. ¹ HNMR spectra of the NBPh	Page 4
Fig. S3. Simulated ¹ HNMR spectra of the NBPh	Page 5
Fig. S4. Simulated ¹ HNMR spectra of the NBPh'	Page 6
Fig. S5. ¹³ CNMR spectra of the NBPh	Page 7
Fig. S6. IR spectra of the NBPh	Page 8
Scheme 1. Two different pathways for the nitration of BPh	Page 9
Fig. S7. Cyclic voltammograms of NBPh in the absence and gradual increasing of BPh	Page 10
Fig. S8. (I) Cyclic voltammograms and (II) of logi-logv of BPh/GIOMC/GC	Page 11
Fig. S9. Cyclic voltammograms of the products resulted from the nitration of catechol	Page 12
Fig. S10. GIOMC in acidic solution	Page 13
Fig. S11: Cyclic voltammograms of catechol and ferrocyanide on the GIOMC/GCE	Page 14

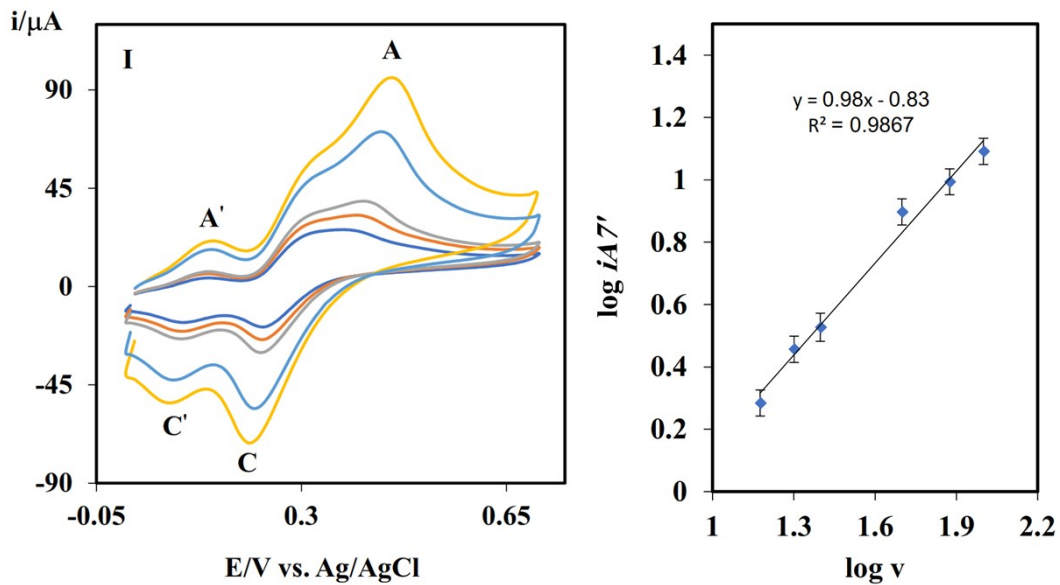


Figure S1: (I) Cyclic voltammograms of 2 mM catechol on GIOMC/GC electrode in aqueous solution with pH of 6 at different scan rates, (II) The plot of logi-logv for voltammograms in Part I. Reference electrode: Ag/AgCl.

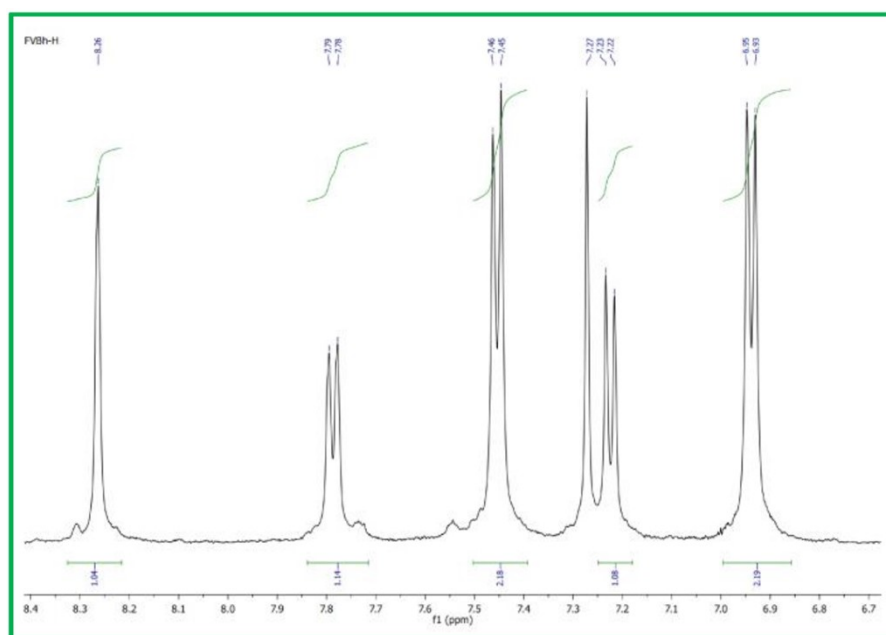
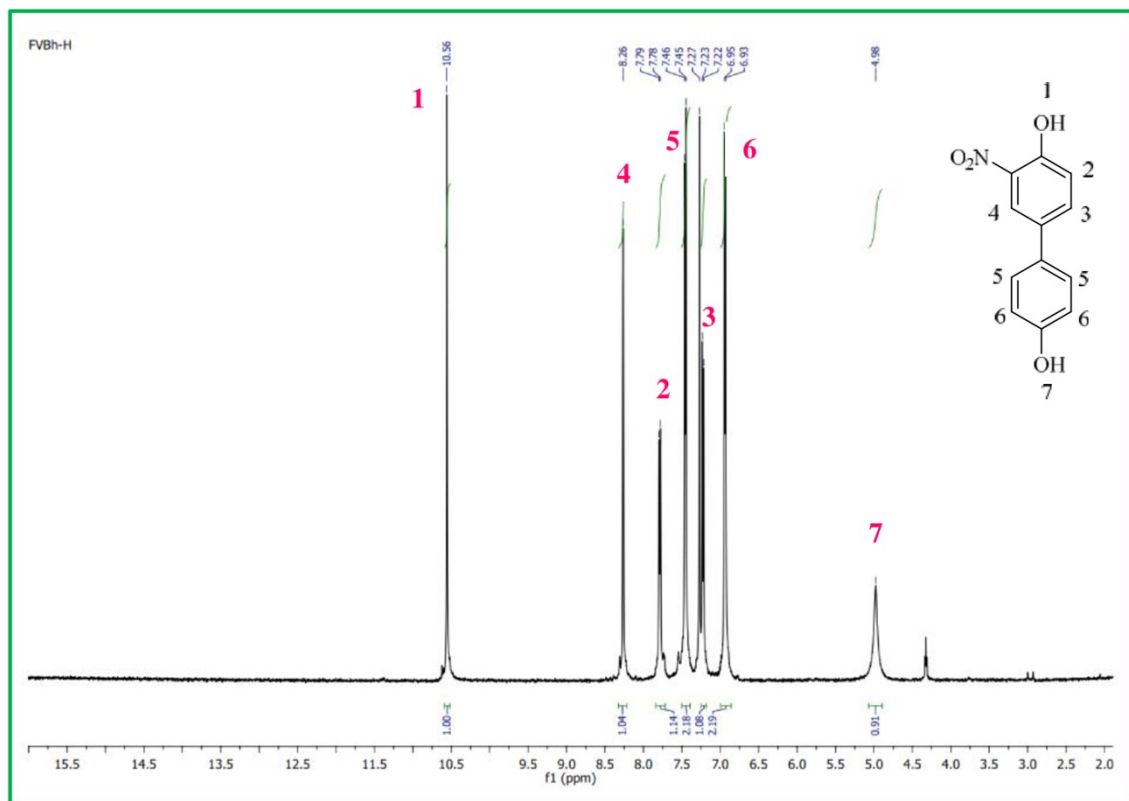


Fig. S2. ¹H NMR spectra of the NBPh

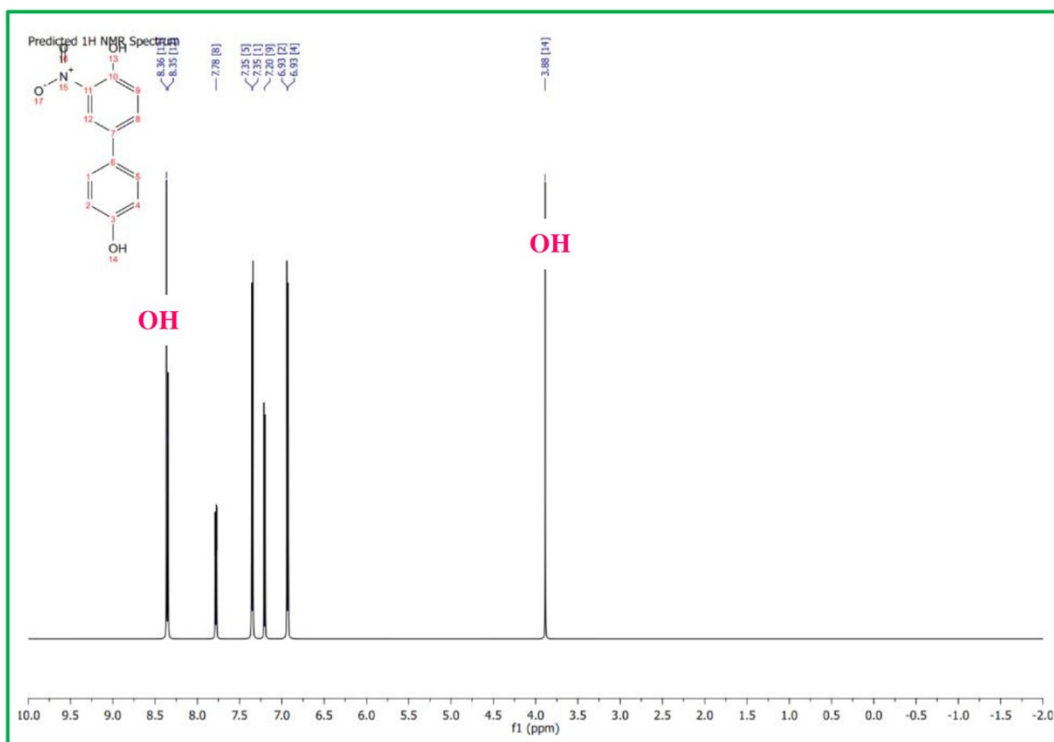


Fig. S3. Simulated ^1H NMR spectra of the NBPh

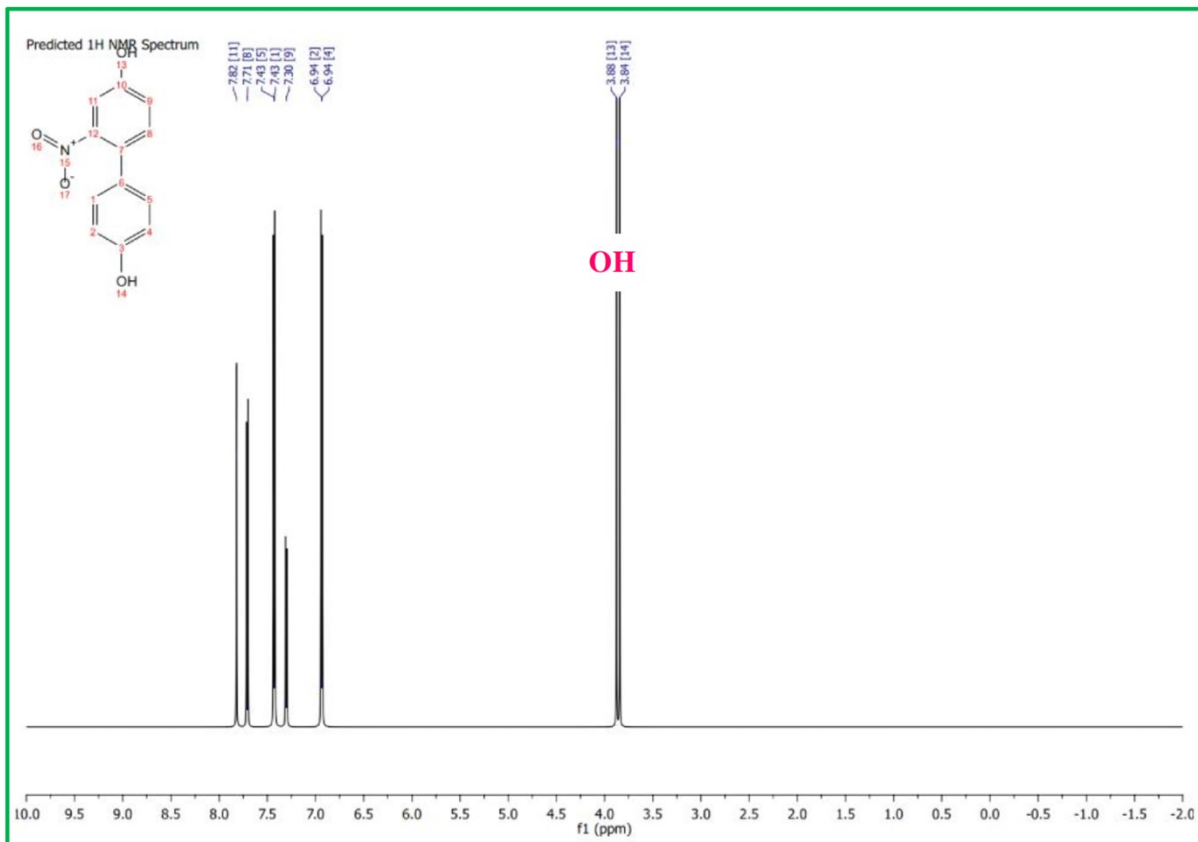


Fig. S4. Simulated ^1H NMR spectra of the NBPh'

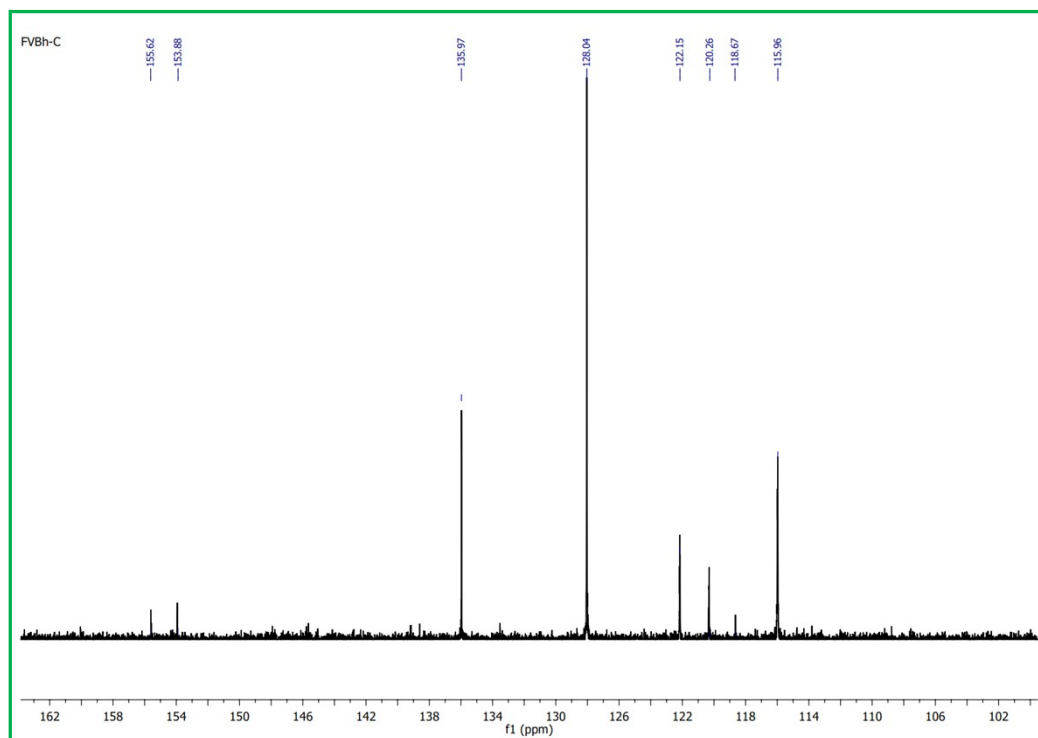
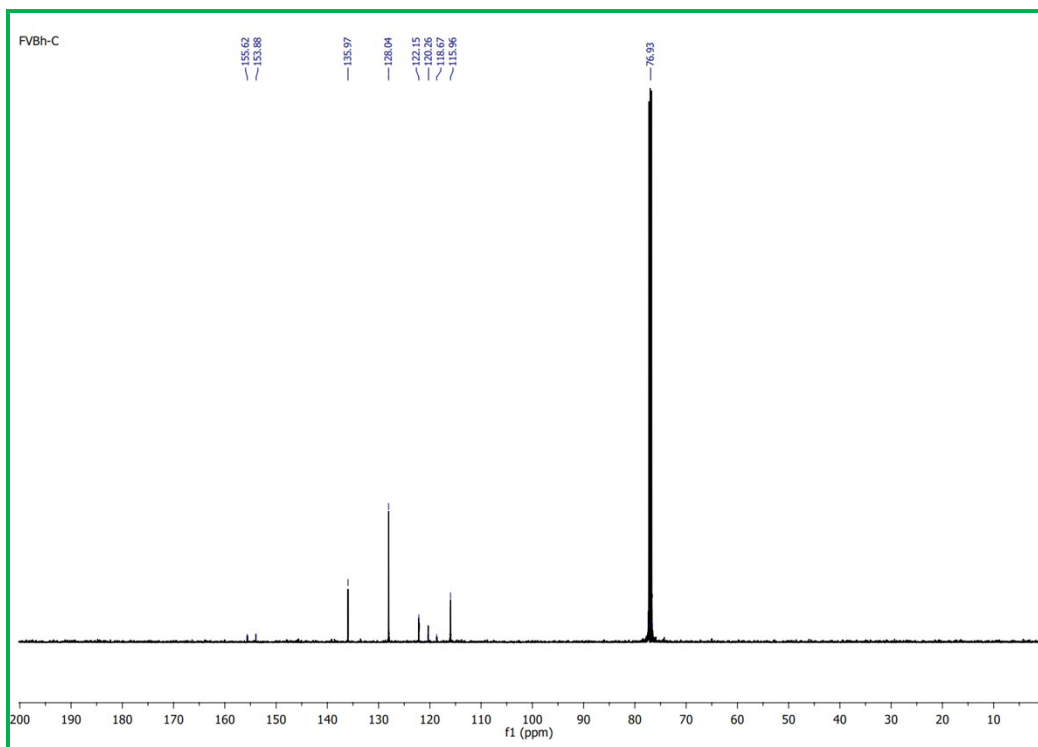


Fig. S5. ^{13}C NMR spectra of the NBPh

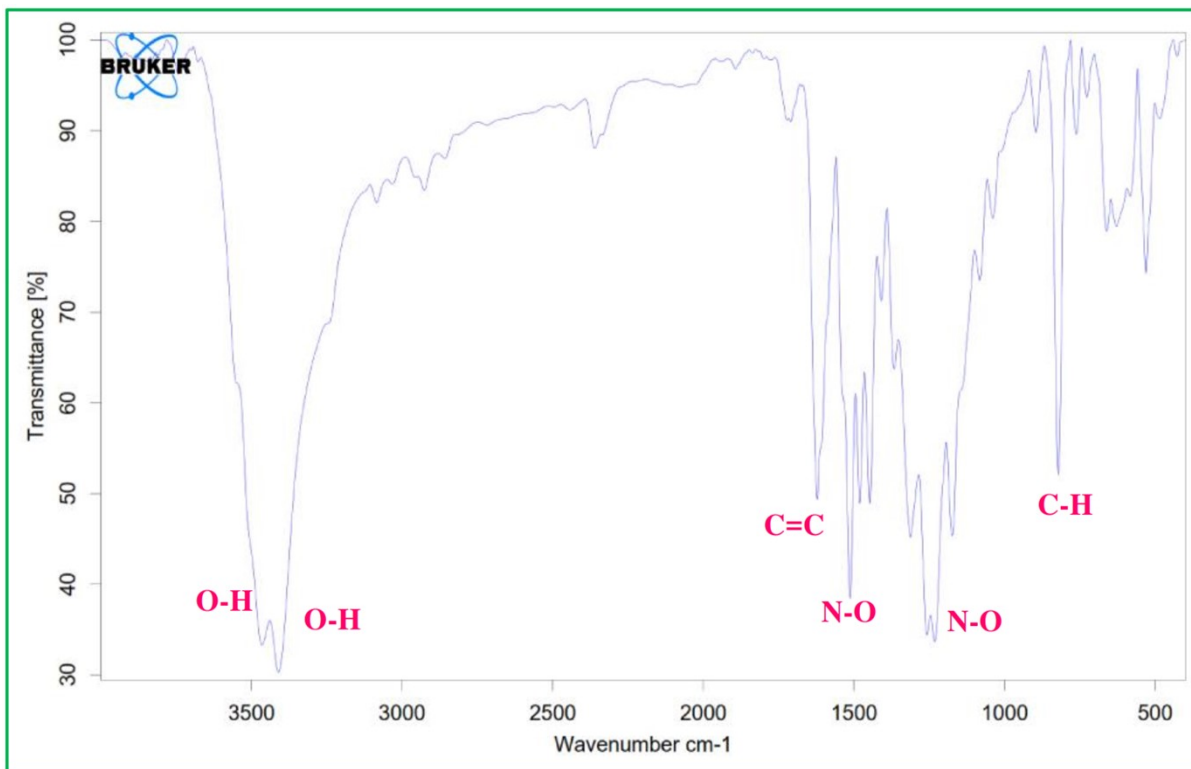
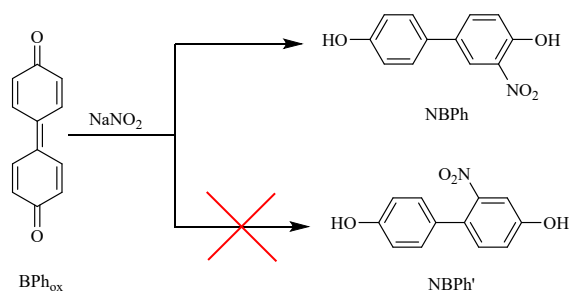


Fig. S6. IR spectra of the NBPh

The product of nitration of BPh was characterized by spectroscopic data (Figs. S2, S5 and S6). The appearance of a singlet signal in $^1\text{H NMR}$ (Fig. 2S) at 8.26 ppm clearly confirms the substitution of a nitro functional group on the phenyl ring. It should also be noted that two possible pathways are considered for nitration of the aromatic ring (Scheme S1). A Comparison between the simulated spectra of NBPh (Fig. S3) and NBPh' (Fig. S4) with the experimental results implies that NBPh has been produced as the final product.



Scheme S1: Two different pathways for the nitration of BPh

In order to make a better comparison between the electrochemical behavior of BPh and NBPh, the voltammetry of 1 mM NBPh was also conducted through the consecutive addition of BPh followed by exerting different potential window from -1 to +0.9 V (Fig. S7I) and 0 to +1 V (Fig. S7II). Appearance and gradual increase the height of A_1/C_1 corresponded to BPh electrode process clearly highlights the notion that the oxidation potential of BPh is to some extent lower than that observed for NBPh. More difficult oxidation of NBPh, as expected, is due to the presence of electron-withdrawing nitro group in close proximity to the redox center of the molecule.

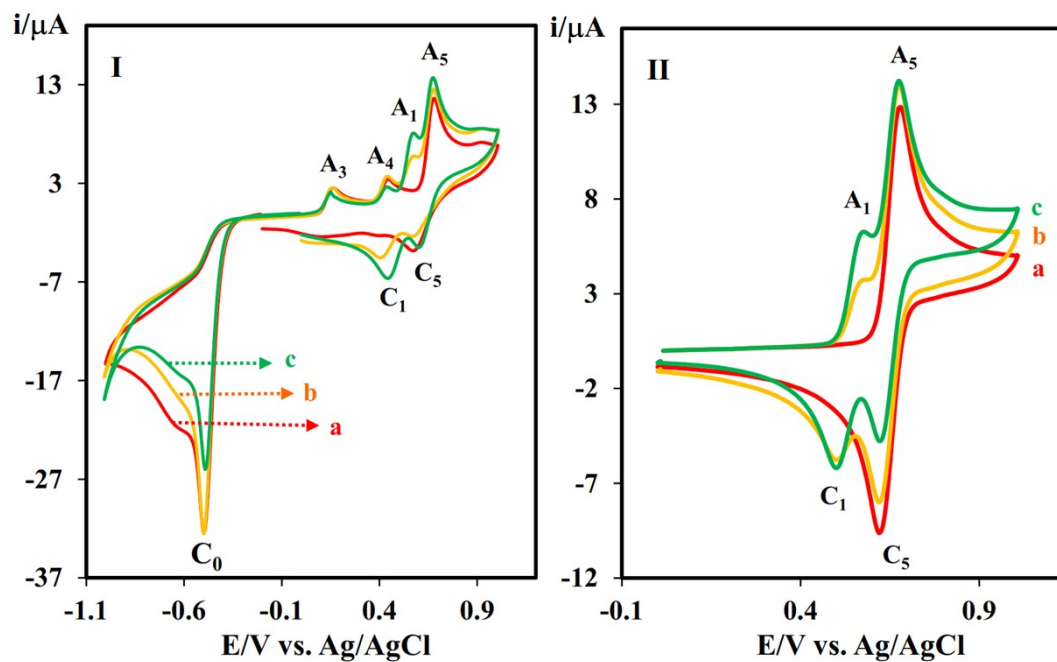


Fig. S7. Cyclic voltammograms of 1 mM NBPh (a) in the absence and (b and c) by gradual increasing of BPh.

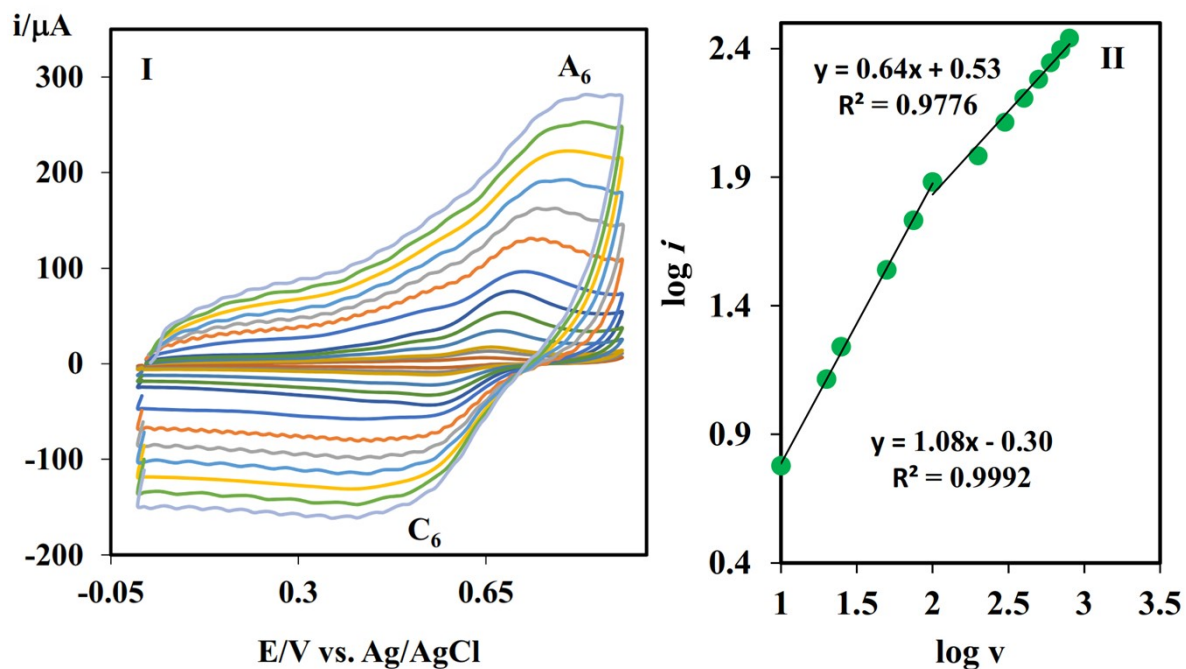


Fig. S8. (I) Cyclic voltammograms of BPh/GIOMC/GC in aqueous phosphate buffer solution at different scan rates, Reference electrode: Ag/AgCl (II) the plot of log i -log v for A_6

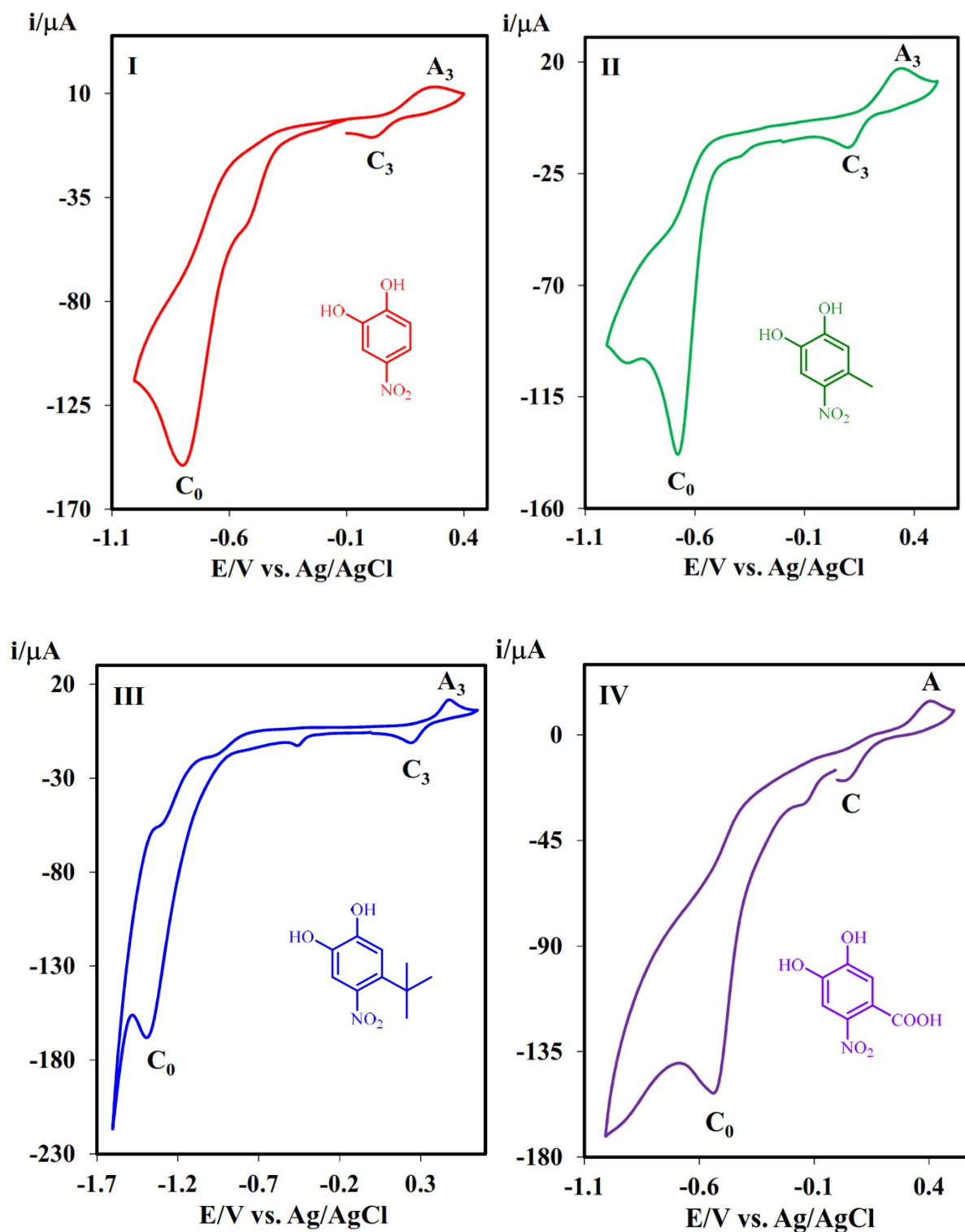


Fig. S9. Cyclic voltammograms of the products resulted from the nitration of catechols,

Reference electrode: Ag/AgCl

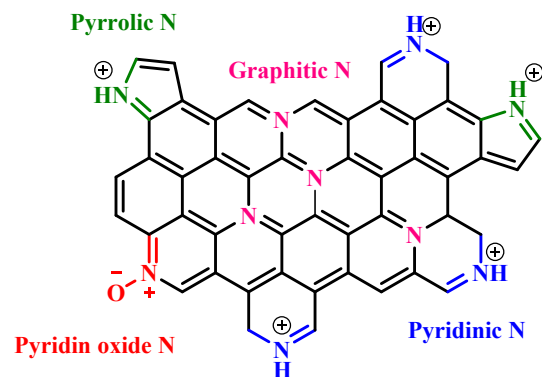


Fig. S10. GIOMC in acidic solution

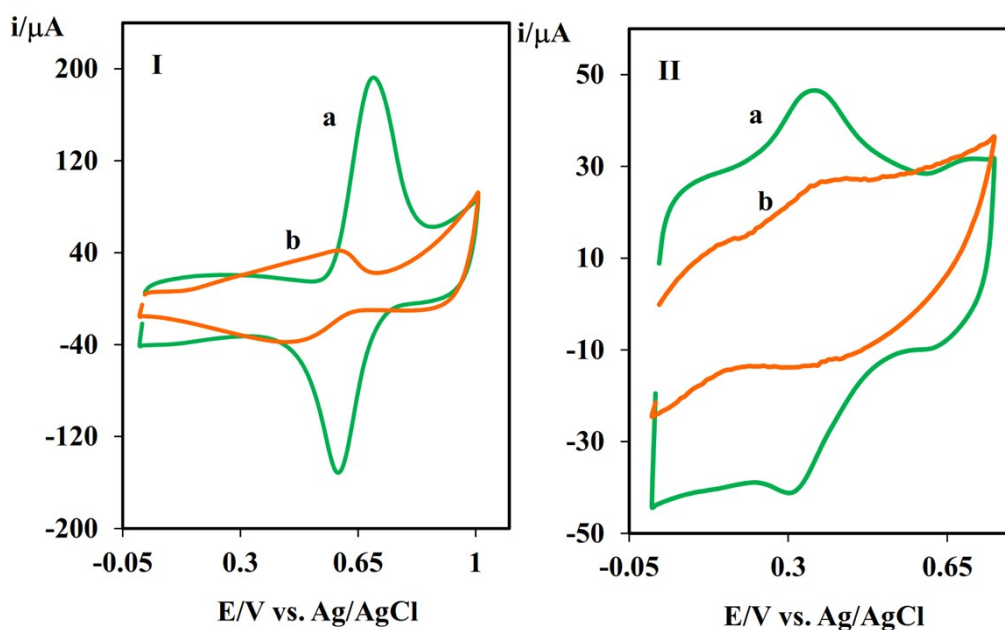


Fig. S11: Cyclic voltammogram of 2 mM solution of I) catechol, II) ferrocyanide on the electrode surface modified with GIOMC in a) 0.1 M HCl solution and b) 0.1 M KCl solution, Reference electrode: Ag/AgCl.